Stabilization mechanisms of a supercritical hydrogen / oxygen flame

By Raphaël Mari†, Bénédicte Cuenot†, Florent Duchaine† AND Laurent Selle‡

The design and optimization of liquid-fuel rocket engines is a major scientific and technological challenge. Despite some sixty years of continuous development, basic features such as flame length, flame stabilization, ignition or the occurrence of combustion instabilities are still difficult to predict. The numerical simulation of such flows is made particularly challenging by the extreme thermodynamic conditions. The pressure in the combustion chamber is usually much larger than the critical pressure of the mixture, resulting in both modeling and numerical issues that are not encountered at ambient conditions. In this paper, numerical simulations of H_2/O_2 transcritical flames that account for all this complexity, are presented in detailed numerical simulations. First, the structure of the flame is analyzed: despite being mostly a diffusion flame, a peculiar structure involving the oxidization of dissociated products is highlighted. Then the influence of a design parameter is studied: it is shown that the thickness of the injector lip has a significant impact on the heat-release rate. Finally, preliminary computations of conjugate heat transfer are presented. Because of the high reactivity of hydrogen, the flame position is weakly affected, despite significant preheating of the reactants by the hot injector lip.

1. Introduction

Most high-performance propulsion devices such as turbines, rocket engines or scramjets have been and are being developed through a costly trial-and-error process. The know-how accumulated over the years by designers and engineers is considerable. Nevertheless, a fundamental understanding of the mechanisms at play is necessary for further gains in performance, safety, fuel efficiency and pollutant emissions. One of the key areas for improvement is to investigate the processes through which the flame is stabilized in the combustion chamber. Indeed, flame stabilization has a direct influence on the robustness and reliability of the engine. Performance, operating range and also combustion instabilities are massively affected by the dynamics of the flame root, which is driven by a large number of parameters: pressure, temperature, fuel composition and combustion regime, just to name a few.

The present study addresses the stabilization of a hydrogen / oxygen flame in a Liquid-fuel Rocket Engine (LRE). Nevertheless, the methodology can be applied to most combustion-based propulsion engines. The specificity of LREs is that they operate at very high pressure for which the thermodynamic properties depart from that of an ideal gas. Indeed, beyond a certain point, called the *critical point*, of coordinates (P_c, T_c), the distinction between gaseous and liquid phases vanishes. This state of matter is called supercritical and under these conditions, phase change is replaced by a steep but continuous variation of the density and thermodynamic properties.

† CERFACS, Toulouse, France
‡ CNRS; IMFT; F-31400 Toulouse, France

Significant experimental and computational efforts were conducted in earlier work, in order to understand and model flame stabilization mechanisms. However, most of these studies were conducted at atmospheric pressure, which is not always representative of the operating conditions of the engine. In the case of LREs, the experiments are dissuasively expensive and the precision of modern laser diagnostics is hindered by the density gradients encountered in supercritical conditions. For these reasons, there are only a few experimental setups operating at supercritical pressure and they are facing tremendous difficulties to retrieve quantitative local diagnostics.

Our objective is to address flame stabilization with high-fidelity numerical simulations under thermodynamic conditions that are typical of a real engine. The goal of this study is to use a two-dimensional Direct Numerical Simulation with:

(*a*) **Detailed chemistry**: At the onset of the chemical reaction, detailed kinetics may play an important role. A kinetic scheme accounting for 8 species and 12 reactions is used (Boivin *et al.* 2011).

(*b*) **Conjugate heat transfer**: In LREs, the propellant are injected at a very low temperature (typically 100 to 150 K) while the burnt gases reach temperatures as high as 3800 K. Therefore, the influence of conjugate heat transfer at the lip of the injector on the stabilization of the flame have to be assessed.

There is a significant body of work on flame stabilization at atmospheric pressure. Carefully instrumented experiments (Cabra *et al.* 2002; Su *et al.* 2006) and high-fidelity numerical simulations (Yamashita *et al.* 1996; Briones *et al.* 2006; Yoo *et al.* 2009) have allowed significant progress. Nevertheless, there is still a controversy on the details of the mechanisms at play for turbulent flames (see Lyons (2007) for a review on the topic).

In the field of LREs, there are only a few studies that address flame stabilization. On the experimental side, the Mascotte bench operated at ONERA was instrumented with simultaneous OH PLIF and OH* light emission (Candel *et al.* 2006; Singla *et al.* 2006, 2007). Close-up views of the injector revealed that the flame was stabilized near the lip and seemed to oscillate because of turbulence. Numerical studies of flame stabilization in LREs are scarce. A few groups started investigating this issue in the late nineties (Oefelein & Yang 1998) and this effort was continued over the past ten years (Juniper & Candel 2003; Oefelein 2005; Zong & Yang 2007). All these studies highlight the influence of the thickness of the lip of the injector and the associated flow dynamics.

The modeling requirements for the numerical simulation of flows under supercritical thermodynamic conditions are fairly well known (Bellan 2000). They essentially consist in using a non-linear equation of state and a consistent modification of the thermodynamic and transport coefficients (Okong'O *et al.* 2002; Meng & Yang 2003). As for combustion modeling, recent work on laminar and turbulent flames have proposed consistent and accurate formalisms with detailed kinetic schemes (Palle & Miller 2007; Ribert *et al.* 2008; Giovangigli *et al.* 2011). However, the peculiarity of supercritical flows is that the variations of state variables and thermodynamic properties are highly non-linear, resulting in steep gradients that require very fine grid resolutions. Recent work at IMFT and CERFACS (Schmitt *et al.* 2010; Ruiz & Selle 2011) has shown that this issue may be one of the weak points of most studies of supercritical flows.

The paper is organized as follows: the configuration and methodology are presented in Sec. 2, then the structure of the turbulent diffusion flame is scrutinized in Sec. 3. Section 4 is devoted to the study of the influence of a design parameter: the height of the splitter plate. Finally, the code coupling to resolve conjugate heat transfer is based on
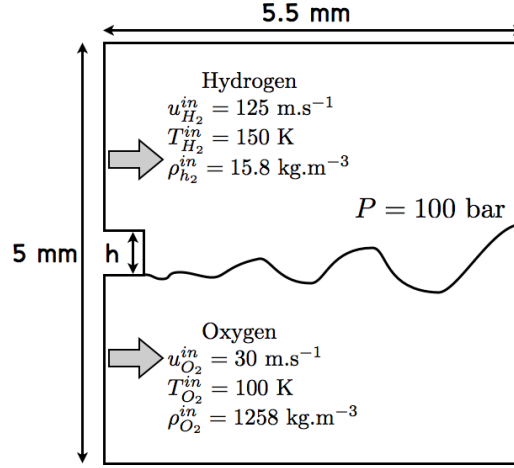
FIGURE 1. Two-dimensional splitter-plate configuration.

the work of Duchaine *et al.* (2009) and is applied for the first time to flame stabilization in supercritical flows (Sec. 5).

2. Configuration and methodology

The configuration is a two-dimensional H_2/O_2 flame stabilized behind a splitter plate at a mean pressure of 100 bar. The computational domain, presented in Fig. 1, is 5.5 mm long in the x-direction and 5.0 mm wide in the y-direction. The splitter-plate height is either $h = 0.5$ mm or $h = 0.1$ mm. Hydrogen is injected above the splitter at a temperature $T_{H_2}^{in} = 150$ K and a bulk velocity $u_{H_2}^{in} = 125$ m/s. Below the splitter, oxygen is fed at $T_{O_2}^{in} = 100$ K and $u_{O_2}^{in} = 30$ m/s. These conditions were chosen to mimic a typical liquid rocket engine, at the nominal operating point. The shape of the inlet velocity profiles follows a 1/7th power law. Although developed turbulence is generally present in the feeding lines of rocket engines, here, no velocity perturbation is added through the inflow boundary condition. Nevertheless, strong turbulence levels caused by vortex shedding are observed downstream the splitter allowing for a developed turbulent mixing layer and strong flame / turbulence interactions (*cf.* Sec. 4). The outlet boundary condition is derived from the NSCBC technique (Poinsot & Lele 1992; Baum *et al.* 1995) and accounts for both real-gas effects (Okong'O & Bellan 2002) and transverse terms (Lodato *et al.* 2008). With a procedure similar to that of Bogey *et al.* (2011), a sponge layer of thickness 0.5 mm is imposed at the exit of the computational domain to prevent spurious oscillations when the strong density gradients hit the boundary. The upper and lower boundaries are treated as symmetries while the splitter is a no-slip wall. The mesh resolution is $\Delta = 1$ μm in a 1.5 mm layer around the splitter. Outside this zone, a transverse stretching factor of approximately 1.02 is employed. The mesh contains approximately 12 million hexahedral cells.

The simulations are performed with the AVBP code developed by CERFACS and IFPEN (`www.cerfacs.fr/cfd/avbp.html`), using a third-order in space and fourth-order in time, two steps Taylor-Galerkin scheme called TTG4A (Quartapelle & Selmin 1993; Colin & Rudgyard 2000). Real-gas thermodynamics is accounted for through the Peng-Robinson equation of state (Peng & Robinson 1976) while transport coefficients are

Parameters	H2	O2	H2O	O	H	OH	H2O2	HO2
$T_{c,i}$ (K)	33	154.581	647.096	105.28	190.82	105.28	141.34	141.34
$P_{c,i}$ (MPa)	1.2838	5.0430	22.064	7.0882	31.013	7.0883	4.7861	4.7861
$V_{c,i}$ (cm^3/mol)	64.284	73.368	55.948	41.205	17.069	41.205	81.926	81.926
ω_{ac}	-0.216	0.0222	0.3443	0.0	0.0	0.0	0.0	0.0
Schmidt Number	0.28	0.99	0.77	0.64	0.17	0.65	0.65	0.65

TABLE 1. Species critical-point properties (temperature T, pressure P, molar volume V and acentric factor ω) and Schmidt numbers.

modeled based on the theory of corresponding states for the dynamic viscosity and the thermal conductivity (Chung *et al.* 1984) and constant Schmidt numbers (*cf.* Tab. 1). The combustion of hydrogen and oxygen is modeled with a skeletal mechanism accounting for 8 species and 12 reactions developed by Boivin *et al.* (2011). Finally, these numerical simulations are DNS in the sense that neither turbulence, nor turbulent-combustion models were used.

3. Flame structure

Given the setup of Fig. 1, when attached to the splitter, the flame developing downstream has a diffusion flame structure. However, it is not clear wether partial premixing or local extinction, for example, can occur. The flame is classically described with a mixture fraction, Z_H, based on the conservation of the H-atom:

$$Z_H = W_H \left(2 \frac{Y_{H_2}}{W_{H_2}} + \frac{Y_H}{W_H} + 2 \frac{Y_{H_2O}}{W_{H_2O}} + \frac{Y_{HO}}{W_{HO}} + \frac{Y_{HO_2}}{W_{HO_2}} + 2 \frac{Y_{H_2O_2}}{W_{H_2O_2}} \right) \qquad (3.1)$$

Scatter-plots of temperature and heat release rate in mixture fraction space are presented in Figs. 2 to 4 for $h = 0.1$ mm in three regions, which are highlighted by square boxes in Fig. 5. These plots correspond to an instantaneous flow field. The same conclusions hold for the thicker splitter and are not shown.

(*a*) **Box 1**: from the splitter to 0.5 mm downstream (Fig. 2). This is the flame anchoring region. The temperature scatter plot shows that there are no points on the mixing line, indicating that the flame is ignited everywhere and no premixing occurs. The broadening of the temperature versus mixture fraction is caused by variable stretch rates and finite-rate chemistry. The heat release rate peaks at the stoichiometric mixture fraction ($Z_H = 0.11$), which is consistent with a diffusion flame structure, but also around $Z_H = 0.03$ *i.e.* in very lean conditions. This flame structure is very peculiar and will be studied in more detail in Box 3.

(*b*) **Box 2**: a region where turbulence is developed (Fig. 3). The flame is highly wrinkled and local extinction by turbulence is most likely. Nevertheless, the temperature scatter plot again shows no points on the mixing line. The heat release rate peaks at the stoichiometric value but the lean secondary peak is still visible. Overall, the flame structure is very similar to that in Box 1 but the combustion is more intense, which is revealed by the higher values of the heat release rate.
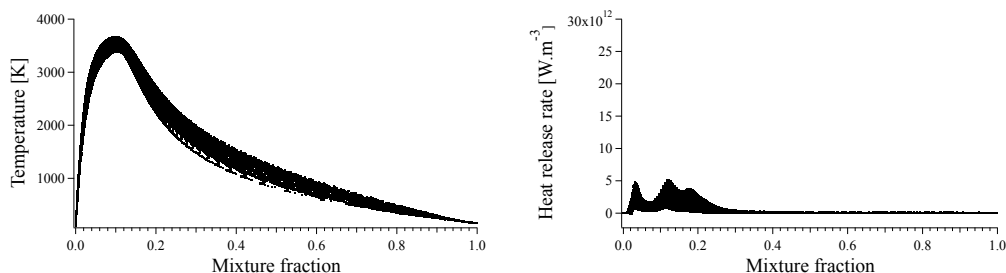
FIGURE 2. Flame structure in Box 1 (*cf.* Fig. 5): temperature and heat release rate scatter plots versus mixture fraction Z_H.
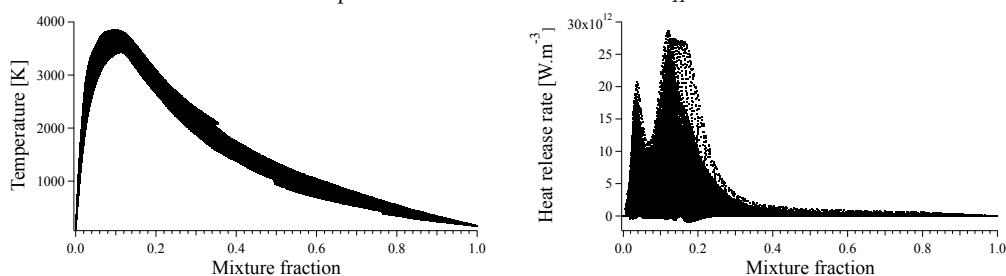
FIGURE 3. Flame structure in Box 2 (*cf.* Fig. 5): temperature and heat release rate scatter plots versus mixture fraction Z_H.
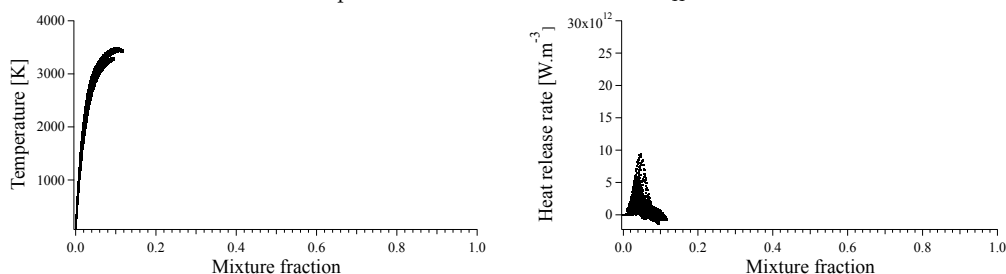
FIGURE 4. Flame structure in Box 3 (*cf.* Fig. 5): temperature and heat release rate scatter plots versus mixture fraction Z_H.

(*c*) **Box 3**: a small pocket of weak combustion close to a strong flame (Fig. 4). With a diffusion flame, one would expect a single reacting sheet corresponding to the stoichiometric flame. The flame structure of this region turns out to be representative of the lean peak of heat release rate in the mixture fraction space observed in Box 1 and Box 2. The study of a temporal animation indicates that it corresponds to a pocket of burnt gases engulfed into cold oxygen. For this flame, the presence of reaction rate at the boundary between burnt gases and pure oxygen is a combined effect of complex chemistry and the high temperature in supercritical H_2/O_2 flames. Indeed, around 3800 K, which is the burnt gases temperature in this case, the reaction is not complete, even for a stoichiometric flame. A fraction of the water dissociates in OH, H and H_2 so that further heat release can occur when in contact with oxygen. It was checked using the CHEMKIN package (private communication with Pr. L. Vervisch) that the composition of the pocket in Box 3 was consistent with the chemical equilibrium of a stoichiometric flame.
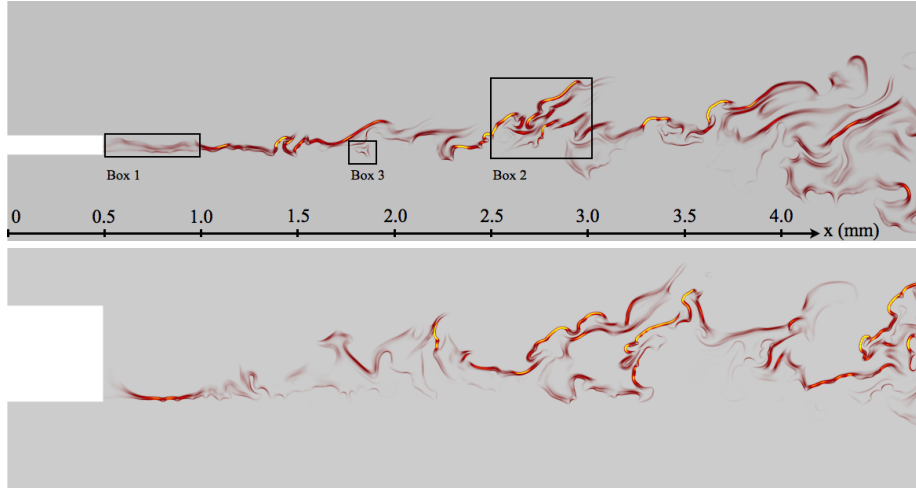
FIGURE 5. Instantaneous field of heat release rate for the two splitter height. Top: $h = 0.1$ mm; bottom: $h = 0.5$ mm.

4. Influence of a design parameter: the splitter height

The thickness of the inner tube separating the oxygen stream from the outer hydrogen flow is a very important design parameter. In a real injector, a thinner tube allows for lower oxygen velocity, therefore increasing the ratio of momentum flux between the two streams. This ratio is known to have a first-order impact on the flame anchoring and total length, for example Singla *et al.* (2005, 2006). Conversely, a thicker tube will have more mechanical and thermal resistance. Two variations of the present configuration are considered: one with a splitter-plate thickness $h = 0.5$ mm and one with $h = 0.1$ mm. These values cover the range of what is encountered in a real engine. However, the present simulations are conducted with equal ratio of momentum flux in order to vary one parameter at a time. In order to give a qualitative representation of the influence of h on the flow field, instantaneous fields of heat release rate are presented in Fig. 5. Overall, the two snapshots are very similar: both configurations exhibit a greatly convoluted flame front for $x > 1$ mm, showing that comparable levels of turbulence develop with the combined effects of bluff-body wake and shear-layer instability. However, close to the splitter plate, the flame brush is thinner for the thick splitter.

Because this could be an artifact of the specific instant chosen for the visualization, averaged quantities are now considered. The relation proposed by Papamoschou & Roshko (1988) estimates that for the configuration of Fig. 1, the convective velocity of the vortical structures is $U_c \simeq 40$ m.s^{-1}. Consequently, the convective time over the 4.5 mm downstream the splitter plate (the last 0.5 mm of the domain are not considered because of the sponge layer) is $\tau_c = 112.5$ μs. The cross-stream average of the heat release rate versus the streamwise coordinate x is presented in Fig. 6 (a). The averaging time is $2\ \tau_c$ for the $h = 0.1$ mm case and $5.6\ \tau_c$ for the $h = 0.5$ mm case. The early development of the flame is very similar for both splitter heights for $x < 2$ mm, with a slight advantage in terms of intensity for the thinner splitter. Past $x = 2$ mm, the thick splitter shows a strong change of slope while the thin splitter exhibits a steady increase in heat release rate. The cross-stream average of the transverse velocity fluctuations presented in Fig. 6 (b) shows that because of an enhanced bluff-body effect, the thick splitter generates higher levels of turbulence. This turbulence is favorable for the flame, however, because the

(a) Heat release rate. (b) Transverse velocity fluctuations (rms).
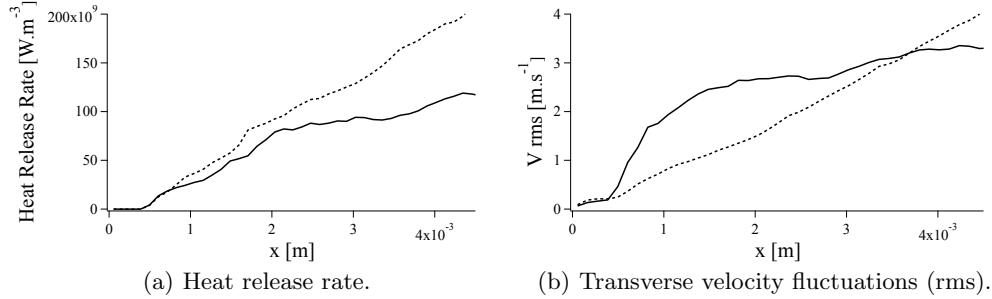
FIGURE 6. Cross-stream averages. ——— $h = 0.5$ mm; - - - - $h = 0.1$ mm.
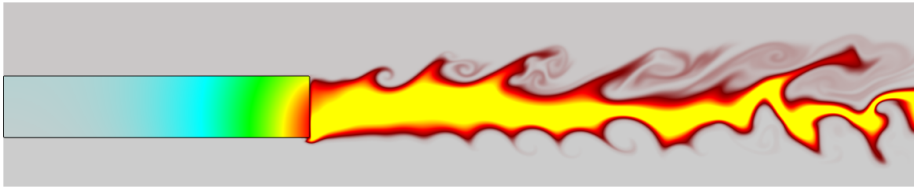
FIGURE 7. Coupled simulation: temperature in the flow (from 100 K to 3800 K) and in the splitter plate (from 100 K to 900 K).

thin splitter has a larger strain rate (same velocity difference over a shorter distance), both configurations have similar combustion intensity. However, around $x = 2$ mm, the velocity fluctuations plateau for the thick splitter while still increasing for the thin one. This is a possible explanation for the concomitant tampering of the combustion intensity in Fig. 6 (a).

5. Coupled simulations

The simulations of Secs. 3 and 4 were performed with an adiabatic boundary condition at the splitter plate. The zero heat flux condition is inadequate to describe the region closest to the wall. A more realistic approach is to consider simultaneous and coupled fluid and solid heat transfer. In this work conjugate heat transfer is performed by running in parallel two solvers (one for the fluid and one for the material) which exchange boundary conditions at the solid surface, using the coupling chain AVBP-AVTP developed at CERFACS with the code coupler OpenPALM (Piacentini *et al.* (2011)) has been used here. The reader is referred to the work of Duchaine *et al.* (2009) for technical details and methodology.

Because the characteristic times of heat transfer in the fluid and the solid are separated by orders of magnitude, as a first step, the problem is considered quasi-steady: the solid is only sensitive to the mean fluxes from the fluid, not to the high-frequency oscillations. As described by Duchaine *et al.* (2009), it is possible, in this case, to speed-up the convergence of the coupled simulation by desynchronizing the time scales in the two codes. In the present simulations, the coupling interval corresponds to $11 \cdot 10^{-6}$ s in the solid and $1.25 \cdot 10^{-9}$ s in the fluid. To avoid interpolation error, the spatial resolution in the solid is identical to that in the fluid ($\Delta = 1 \ \mu$m). This leads to cell size smaller than necessary, but the computational time for the resolution of the solid remains negligible: 1021 CPUs are used for the fluid and only 2 for the solid. One CPU is also dedicated to the scheduling of the coupled application.

The temperature fields obtained with the coupled simulation in both the fluid and the solid are presented in Fig. 7. The temperature in the splitter plate reaches 900 K at its tip but rapidly decreases upstream because of the low temperature of the reactants with which it is in contact. The temperature gradient is almost zero at the upstream boundary condition, which is an a posteriori indication that the splitter length is sufficient to apply a fixed temperature boundary condition. The temperature in the fluid, however, is only marginally affected by the heat loss at the solid boundary. Indeed, hydrogen is so reactive that the flame position is virtually unchanged. Nevertheless, this could be an artifact of the quasi-steady approximation and will require further investigation. Another point that will require further work is the analysis of the preheating of the reactants in contact with the hot splitter and its influence on the flow field and the flame structure.

6. Conclusion

This work presents the results of Direct Numerical Simulations of a hydrogen / oxygen flame under supercritical thermodynamic conditions, typical of a liquid rocket engine. First the structure of the flame was analyzed in the mixture fraction space. It is shown that neither partial premixing nor local extinction occur, mostly due to the high reactivity of the fuel (H_2). The structure is that of a diffusion flame almost everywhere but a peculiar reaction zone corresponding to a pocket of dissociated burnt gases engulfed in the oxygen stream is uncovered. The influence of a design parameter, the height of the splitter plate, is studied: it is shown that the thinner splitter enhances combustion despite lower levels of turbulence in its wake. Finally, coupled simulations with conjugate heat transfer are conducted. The tip of the splitter plate is heated up by the burnt gases but the location of the flame anchoring and the downstream evolution of the flame are marginally affected.

REFERENCES

BAUM, M., POINSOT, T. & THÉVENIN, D. 1995 Accurate Boundary Conditions for Multicomponent Reactive Flows. *Journal of Computational Physics* **116** (2), 247–261.

BELLAN, J. 2000 Supercritical (and subcritical) fluid behavior and modeling: drops, streams, shear and mixing layers, jets and sprays. *Progress in Energy and Combustion Science* **26** (4-6), 329–366.

BOGEY, C., MARSDEN, O. & BAILLY, C. 2011 Large-eddy simulation of the flow and acoustic fields of a Reynolds number 10[sup 5] subsonic jet with tripped exit boundary layers. *Physics of Fluids* **23** (3), 035104.

BOIVIN, P., JIMÉNEZ, C., A.L. SÁNCHEZ & WILLIAMS, F. 2011 A four-step reduced mechanism for syngas combustion. *Combustion and Flame* **158** (6), 1059–1063.

BRIONES, A. M., AGGARWAL, S. K. & KATTA, V. R. 2006 A numerical investigation of flame liftoff, stabilization, and blowout. *Physics of Fluids* **18** (4), 043603.

CABRA, R., MYHRVOLD, T., CHEN, J., DIBBLE, R., KARPETIS, A. & BARLOW, R. 2002 Simultaneous laser Raman-Rayleigh-LIF measurements and numerical modeling results of a lifted turbulent H2/N2 jet flame in a vitiated coflow. *Proceedings of the Combustion Institute* **29** (2), 1881–1888.

CANDEL, S., JUNIPER, M., SINGLA, G., SCOUFLAIRE, P. & ROLON, C. 2006 Structure and Dynamics of Cryogenic Flames At Supercritical Pressure. *Combustion Science and Technology* **178** (1-3), 161–192.

CHUNG, T.-H., LEE, L. L. & STARLING, K. E. 1984 Application of kinetic gas theories and multiparameter correlation for prediction of dilute gas viscosity and thermal conductivity. *Ind. Eng. Chem., Fundam.* **23**, 8–13.

COLIN, O. & RUDGYARD, M. 2000 Development of High-Order TaylorGalerkin Schemes for LES. *Journal of Computational Physics* **162** (2), 338–371.

DUCHAINE, F., CORPRON, A., PONS, L., MOUREAU, V., NICOUD, F. & POINSOT, T. 2009 Development and assessment of a coupled strategy for conjugate heat transfer with Large Eddy Simulation: Application to a cooled turbine blade. *International Journal of Heat and Fluid Flow* **30** (6), 1129–1141.

GIOVANGIGLI, V., MATUSZEWSKI, L. & DUPOIRIEUX, F. 2011 Detailed modeling of planar transcritical H2-O2N2 flames. *Combustion Theory and Modelling* **15** (2), 141–182.

JUNIPER, M. & CANDEL, S. 2003 Edge diffusion flame stabilization behind a step over a liquid reactant. *Journal of propulsion and power* **19** (3), 332–341.

LODATO, G., DOMINGO, P. & VERVISCH, L. 2008 Three-dimensional boundary conditions for direct and large-eddy simulation of compressible viscous flows. *Journal of Computational Physics* **227** (10), 5105–5143.

LYONS, K. M. 2007 Toward an understanding of the stabilization mechanisms of lifted turbulent jet flames: Experiments. *Progress in Energy and Combustion Science* **33** (2), 211–231.

MENG, H. & YANG, V. 2003 A unified treatment of general fluid thermodynamics and its application to a preconditioning scheme. *Journal of Computational Physics* **189** (1), 277–304.

OEFELEIN, J. 2005 Thermophysical characteristics of shear-coaxial LOX-H2 flames at supercritical pressure. *Proceedings of the Combustion Institute* **30** (2), 2929–2937.

OEFELEIN, J. C. & YANG, V. 1998 Modeling High-Pressure Mixing and Combustion Processes in Liquid Rocket Engines. *Journal of Propulsion and Power* **14** (5), 843–857.

OKONG'O, N., BELLAN, J. & HARSTAD, K. 2002 Direct Numerical Simulations of O/H Temporal Mixing Layers Under Supercritical Conditions. *AIAA Journal* **40** (5), 914–926.

OKONG'O, N. A. & BELLAN, J. 2002 Consistent Boundary Conditions for Multicompo-

nent Real Gas Mixtures Based on Characteristic Waves. *Journal of Computational Physics* **176** (2), 330–344.

PALLE, S. & MILLER, R. 2007 Analysis of high-pressure hydrogen , methane , and heptane laminar diffusion flames: Thermal diffusion factor modeling. *Combustion and Flame* **151** (4), 581–600.

PAPAMOSCHOU, D. & ROSHKO, A. 1988 The compressible turbulent shear layer : an experimental study. *Journal of Fluid Mechanics* **197**, 453–477.

PENG, D.-Y. & ROBINSON, D. B. 1976 A New Two-Constant Equation of State. *Ind. Eng. Chem., Fundam.* **15** (1), 59–64.

PIACENTINI, A., MOREL, T., THEVENIN, A. & DUCHAINE, F. 2011 Open-palm: an open source dynamic parallel coupler. In *In IV International Conference on Computational Methods for Coupled Problems in Science and Engineering*.

POINSOT, T. & LELE, S. 1992 Boundary conditions for direct simulations of compressible viscous flows. *Journal of Computational Physics* **101** (1), 104–129.

QUARTAPELLE, L. & SELMIN, V. 1993 High-order Taylor-Galerkin methods for nonlinear multidimensional problems.

RIBERT, G., ZONG, N., YANG, V., PONS, L., DARABIHA, N. & CANDEL, S. 2008 Counterflow diffusion flames of general fluids : Oxygen / hydrogen mixtures. *Combustion and Flame* **154**, 319–330.

RUIZ, A. & SELLE, L. 2011 Simulation of a turbulent supercritical hydrogen/oxygen flow behind a splitter plate: cold flow and flame stabilization. In *7th Mediterranean Combustion Symposium*. Chia Laguna, Cagliari, Sardinia, Italy.

SCHMITT, T., SELLE, L., RUIZ, A. & CUENOT, B. 2010 Large-Eddy Simulation of Supercritical-Pressure Round Jets. *AIAA Journal* **48** (9), 2133–2144.

SINGLA, G., SCOUFLAIRE, P., ROLON, C. & CANDEL, S. 2005 Transcritical oxygen/transcritical or supercritical methane combustion. *Proceedings of the Combustion Institute* **30** (2), 2921–2928.

SINGLA, G., SCOUFLAIRE, P., ROLON, C. & CANDEL, S. 2006 Planar laser-induced fluorescence of OH in high-pressure cryogenic LOx/GH2 jet flames. *Combustion and Flame* **144** (1-2), 151–169.

SINGLA, G., SCOUFLAIRE, P., ROLON, J. & CANDEL, S. 2007 Flame stabilization in high pressure LOx/GH2 and GCH4 combustion. *Proceedings of the Combustion Institute* **31** (2), 2215–2222.

SU, L., SUN, O. & MUNGAL, M. 2006 Experimental investigation of stabilization mechanisms in turbulent, lifted jet diffusion flames. *Combustion and Flame* **144** (3), 494–512.

YAMASHITA, H., SHIMADA, M. & TAKENO, T. 1996 A Numerical Study on Flame Stability at the Transition Point of Jet Diffusion Flames. *Proceedings of the Combustion Institute* **26** (1), 27–34.

YOO, C. S., SANKARAN, R. & CHEN, J. H. 2009 Three-dimensional direct numerical simulation of a turbulent lifted hydrogen jet flame in heated coflow: flame stabilization and structure. *Journal of Fluid Mechanics* **640**, 453.

ZONG, N. & YANG, V. 2007 Near-field flow and flame dynamics of LOX/methane shear-coaxial injector under supercritical conditions. *Proceedings of the Combustion Institute* **31** (2), 2309–2317.